Molecular Cell, Volume *78*

Supplemental Information

4D Genome Rewiring during Oncogene-Induced and Replicative Senescence

Satish Sati, Boyan Bonev, Quentin Szabo, Daniel Jost, Paul Bensadoun, Francois Serra, Vincent Loubiere, Giorgio Lucio Papadopoulos, Juan-Carlos Rivera-Mulia, Lauriane Fritsch, Pauline Bouret, David Castillo, Josep Ll. Gelpi, Modesto Orozco, Cedric Vaillant, Franck Pellestor, Frederic Bantignies, Marc A. Marti-Renom, David M. Gilbert, Jean-Marc Lemaitre, and Giacomo Cavalli

Supplementary Figure 1

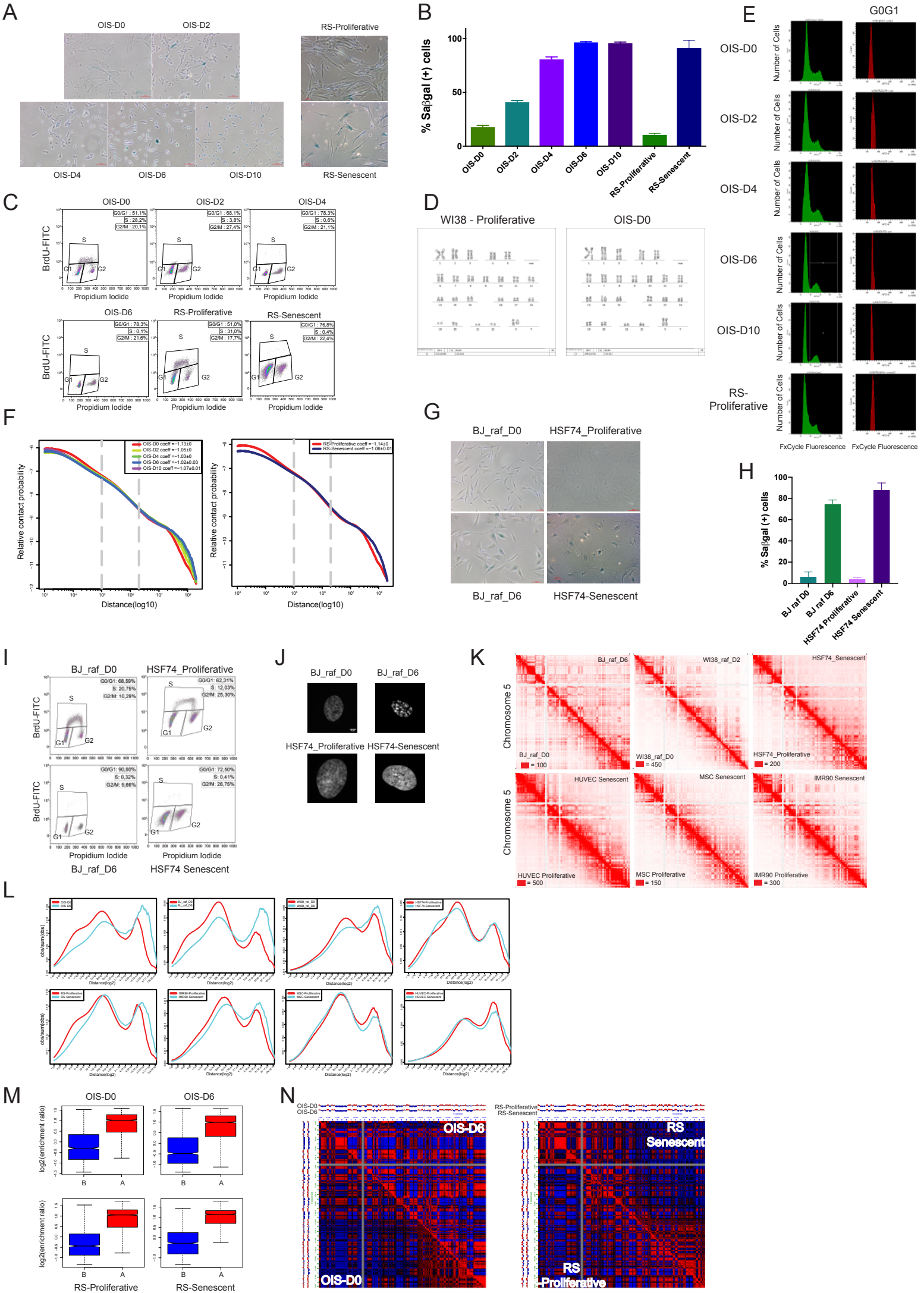

S1. Global changes in chromatin organisation during senescence, Related to Figure 1.

(A) Representative images from the Senescence-Associated β-galactosidase staining in OIS-D0, OIS-D2, OIS-D4, OIS-D6, OIS-D10, RS-Proliferative and RS-Senescent. Scale bar = 100 μm. (B) Percentages of cells stained positive for Senescence-Associated β-galactosidase staining. Data represented as bar plot showing mean ± SD (n = 3). (C) Cell cycle profiles from FACS analyses of pulsed BrdU incorporation versus propidium iodide fluorescence (DNA content) in OIS-D0, OIS-D2, OIS-D4, OIS-D6, RS-Proliferative and RS-Senescent. (D) A representative image of giemsa staining performed on un-induced WI-38 hTERT/GFP-RAF1-ER and WI-38 primary cells showing a normal Karyotype. (E) FACS sorting for cells in G0G1+ phase of the cell cycle in OIS system and for WI-38 primary cells. The upper panel display FACS profile and bottom panel the sorted population. (F) Log-log contact probability as a function of the genomic distance. The exponent γ represents the mean slope ± SD of the best-fit line between 100Kb and 2Mb. (G) Area measurements of Chromosome 5 under proliferative and senescent conditions at different thresholds (as in Figure 1E). (H) Representative images from the Senescence-Associated β-galactosidase staining in BJ raf D0, BJ raf D6, HSF74-Proliferative and HSF74-Senescent cells. Scale bar = 100 μm. (I) Percentages of cells stained positive for Senescence-Associated β-galactosidase staining. Data represented as bar plot showing mean ± SD (n = 3). (J) Cell cycle profiles from FACS analyses of pulsed BrdU incorporation versus propidium iodide fluorescence (DNA content) in BJ raf D0, BJ raf D6, HSF74-Proliferative, HSF74-Senescent (K) Schematic representation (DAPI staining) of the BJ-D0, BJ-D6, HSF74-Proliferative, HSF74-Senescent and HSF92 cells. Only BJ-D6 cells show SAHF bodies. Scale bar = 5 μm. (L) Normalised Hi-C contact maps for chromosome 5 at 500-Kb resolution. For all maps the lower left bottom of individual Hi-C plots represent control cells (D0 or RS-Proliferative) and upper right part displays senescence condition (OIS or RS-Senescent). The maximum intensity for each comparison (panel) is indicated in the lower left corner. (M) Contact probability in logarithmic bins. Lines: mean values from biological replicates. (N) Enrichment for replication timing in the two compartments. (O) Pearson correlation matrix displaying the correlation [from –1 (blue) to +1 (red)] between the intra-chromosomal interaction profiles along chromosome 5. The lower left bottom of individual Hi-C correlation matrix represent control cells (D0 or RS-Proliferative) and upper right part displays senescence condition (D6 or RS-Senescent). The eigenvector are above the Hi-C matrix.

Supplemantary Figure 2

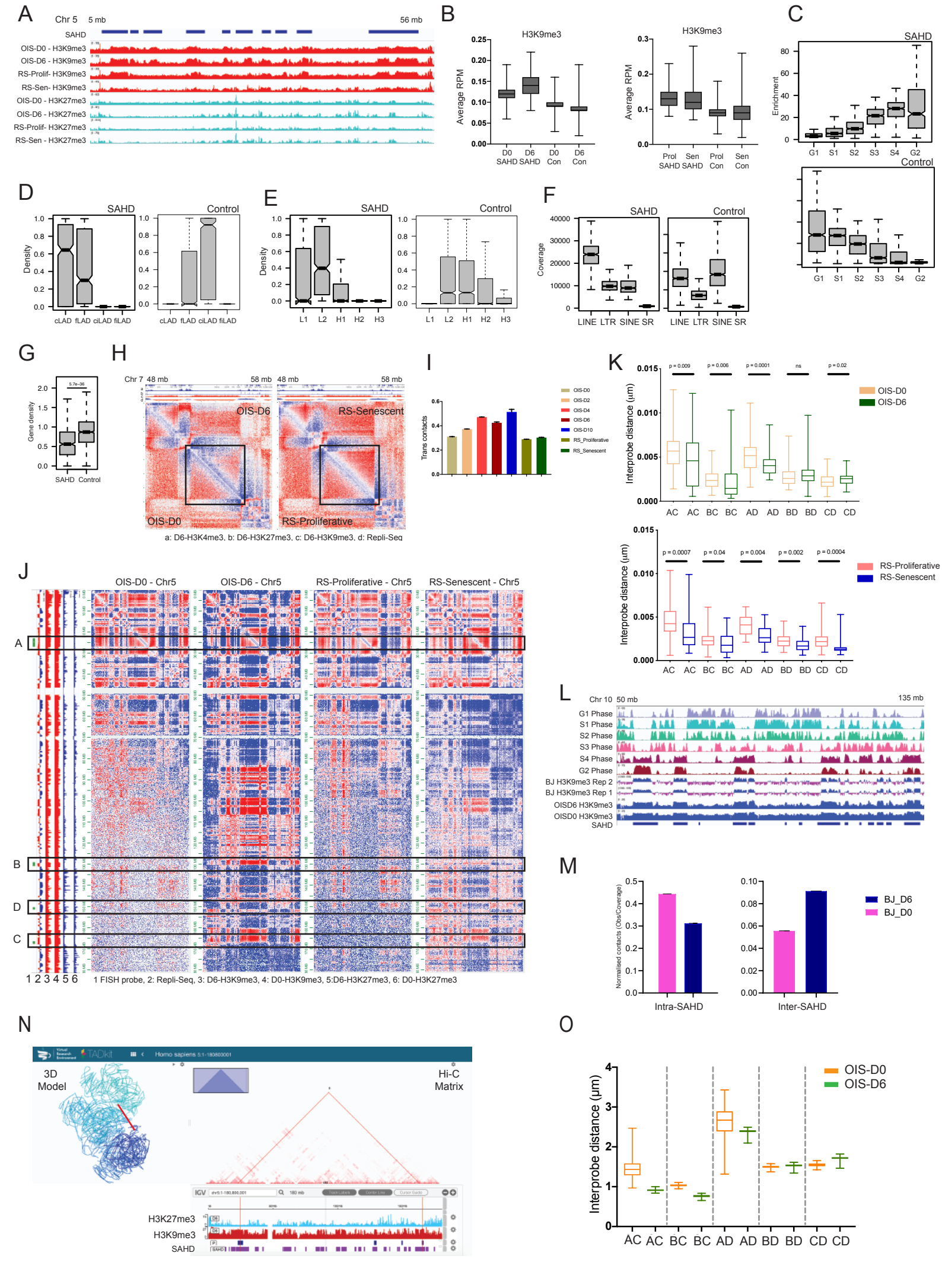

S2. Identification and validation of SAHDs, Related to Figure 2.

(A) IGV genome browser snapshot of the ChIP-Seq profiles of OIS-D0 and OIS-D6 cells displaying the conservation of H3K9me3 and H3K27me3 domains during OIS. (B) Average enrichment of H3K9me3 modification in SAHD and control regions in D0, D6, RS-Proliferative and RS-Senescent. (C) Enrichment of replication timing regions (early replicating - G1, S1, S2, S3, S4, very late replicating -G2) across SAHD and Control regions. (D) Enrichment of different classes of LADs (cLADs, fLADs, ciLADs, fiLADs) across SAHD and Control regions. The regions were taken from Lenain et al. (Lenain et al., 2017). (E) Enrichment of different classes of isochores (L1, L2, H1, H2, H3) across SAHD and Control regions. (F) Enrichment of major repeat classes (LINE, SINE, LTR, Simple repeats) across SAHD and Control regions. (G) Enrichment of Ref-Seq genes across SAHD and Control regions. (H) Representative SAHD regions displaying the ChIP tracks and the observed / expected profiles of the respective datasets. (I) Trans inter-SAHD interactions from OIS and RS samples. Data represented as bar plots showing the mean ± SD. (J) Oligopaint probe design. View of full chromosome 5 - p arm interactions in OIS D0, D6, RS-Proliferative and RS-Senescent maps along with the ChIP profiles. The regions selected for FISH probe designing are highlighted in boxes. (K) Boxplot of inter-probe distances form Figure 2H and 2K, normalised by mean volume in OIS and RS system. Statistical significance is calculated using Mann-Whitney test. (L) IGV genome browser snapshot of the Repli-Seq and ChIP-Seq profiles of BJ cells from ENCODE project and Becker et al (Becker et al., 2017) respectively, along with OIS-D0 and OIS-D6 H3K9me3 profiles in chromosome 10. (M) Quantification of contacts within and between SAHDs in BJ-D0 and BJ-D6 condition. Data showing the mean ± SD. (N) Snapshot of the MuG-VRE displaying, right panel- 3D model from chromosome 5 at 100 kb resolution of OIS-D6 condition, left panel - Hi-C matrix, and bottom panel – ChIP tracks from OIS-D6 and SAHD tracks. The red line in the 3D model highlights the two SAHD positions (A and D), which are also highlighted in the Hi-C matrix. (O) Boxplot of inter-probe distances form calculated from the TADbit 3D models in OIS-D0 and OIS-D6.

Supplementary Figure 3

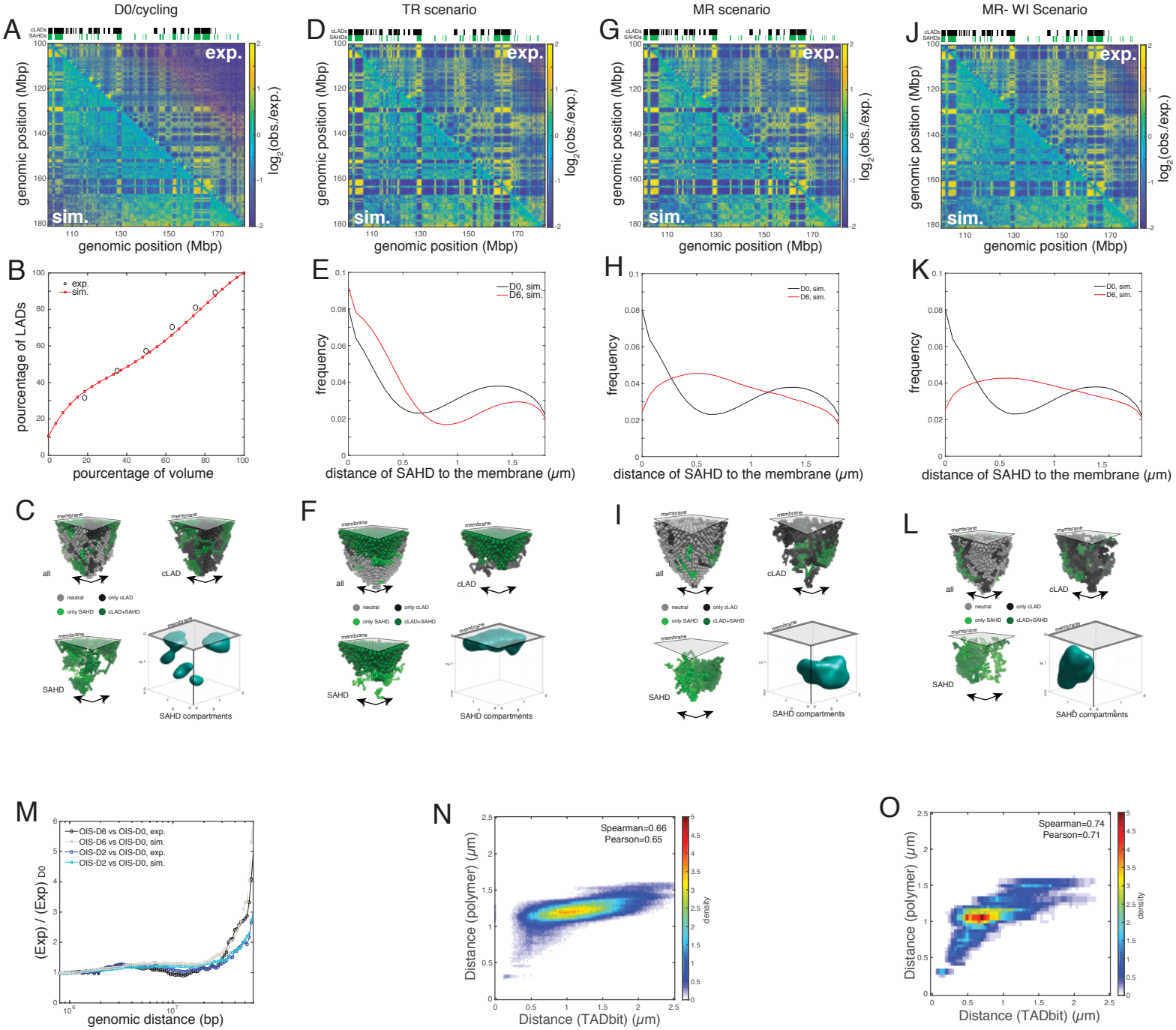

S3. In silico polymer modelling of OIS conditions, Related to Figure 3.

Panels (A) to (C): Inference of a model for cycling/D0 cells. (A) Experimental and simulated maps of the ratio between the observed and expected probability. (B) Cumulative probability to find a LAD in a fraction of the total volume measured starting from the membrane. Experimental data were taken from Kind et al (Kind et al., 2013). (C) Typical snapshot extracted from simulation. We separated cLAD and SAHD monomers and isolated dense SAHD compartments. Panels (D) to (F): Predictions for the time-release (TR) scenario. (D) Experimental and simulated maps of the ratio between the observed and expected probability. (E) Probability distribution function to find a SAHD monomer at a given distance to the membrane. (F) Typical snapshot extracted from simulation. We separated cLAD and SAHD monomers and isolated dense SAHD compartments. Panels (G) to (I): Predictions for the membrane-release (MR) scenario. (G) Experimental and simulated maps of the ratio between the observed and expected probability. (H) Probability distribution function to find a SAHD monomer at a given distance to the membrane. (I) Typical snapshot extracted from simulation. We separated cLAD and SAHD monomers and isolated dense SAHD compartments. Panels (J) to (L): Predictions for the membrane-release with weakening of heterochromatin attraction (MR-WI) scenario. (J) Experimental and simulated maps of the ratio between the observed and expected probability. (K) Probability distribution function to find a heterochromatin monomer at a given distance to the membrane. (L) Typical snapshot extracted from simulation. We separated cLAD and SAHD monomers and isolated dense SAHD compartments. (M) Generic long-range relaxation of chromosome. Ratio between the total average contact probability between any pairs of loci (expected probability) at a given time upon senescence entry and the expected probability for D0 cells as a function of the genomic distance, normalized by the corresponding value at 1Mbp. (N) The correlation between Polymer model (Y axis) and TADbit models (X axis). The X and the Y axes represent distances computed from respective models, between all 100 kb bins, over 80 Mb region on chromosome 5 (100 to 180 Mb). (O) The correlation between Polymer model (Y axis) and TADbit models (X axis). The X and the Y axes represent distances computed from respective models, between all SAHDs lying over the modelled 80 Mb region of chromosome 5 (100 to 180 Mb).

Supplementary Figure 4

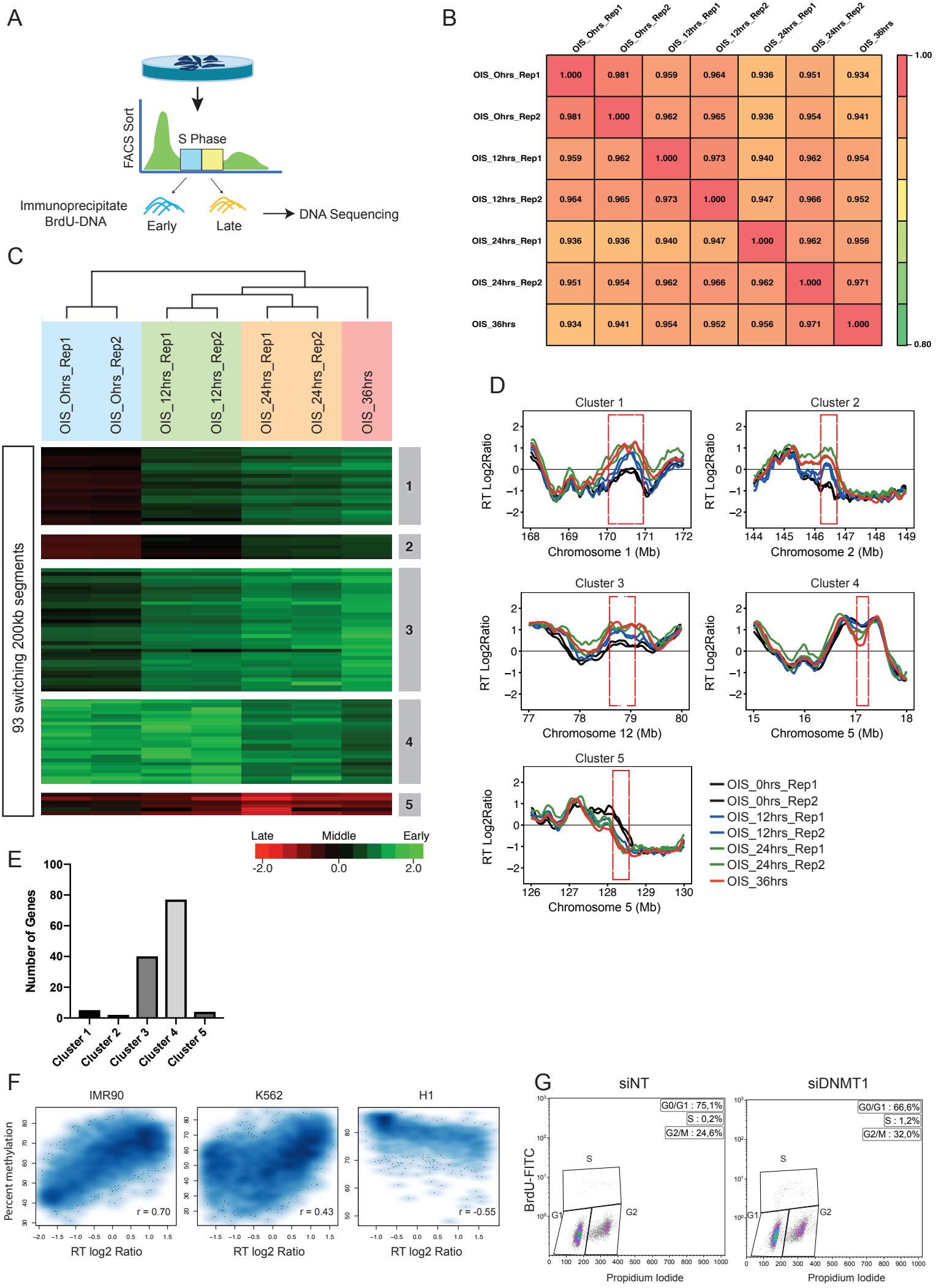

S4. Replication timing and methyl cytosine levels associated with SAHDs, Related to Figure 4.

(A) Schematic overview of the Repli-Seq experiment. Cells pulse labelled with BrdU and sorted into early and late S-phase followed by immunoprecipitation and sequencing. (B) Correlation of genome-wide RT profiles of WI38 RAF cells at early stages of OIS. (C) The differential RT regions (grey boxes 1-5) identified by unsupervised clustering of RT-variable regions. The heat map shows the RT ratios [= log2(early/late)]. (D) Representative examples of RT profile alterations among different clusters in OIS. The positive values correspond to early replication and negative values to late replication. The coloured box highlights the differential RT region. (E) Boxplot displaying number of genes within each individual differential RT cluster. (F) Scatter plot comparing the RT profiles and mC levels (percent methylation) in IMR90, K562 and H1 cells. The RT profiles and mC profiles for IMR90, K562 and H1 cells were downloaded from ENCODE and NCBI Roadmap to epigenomics project. The correlation of the individual datasets is indicated on the bottom right panel. (G) Cell cycle profiles from FACS analyses of pulsed BrdU incorporation versus propidium iodide fluorescence (DNA content) in siSNMT1 and NT treated cells.

Supplementary Figure 5

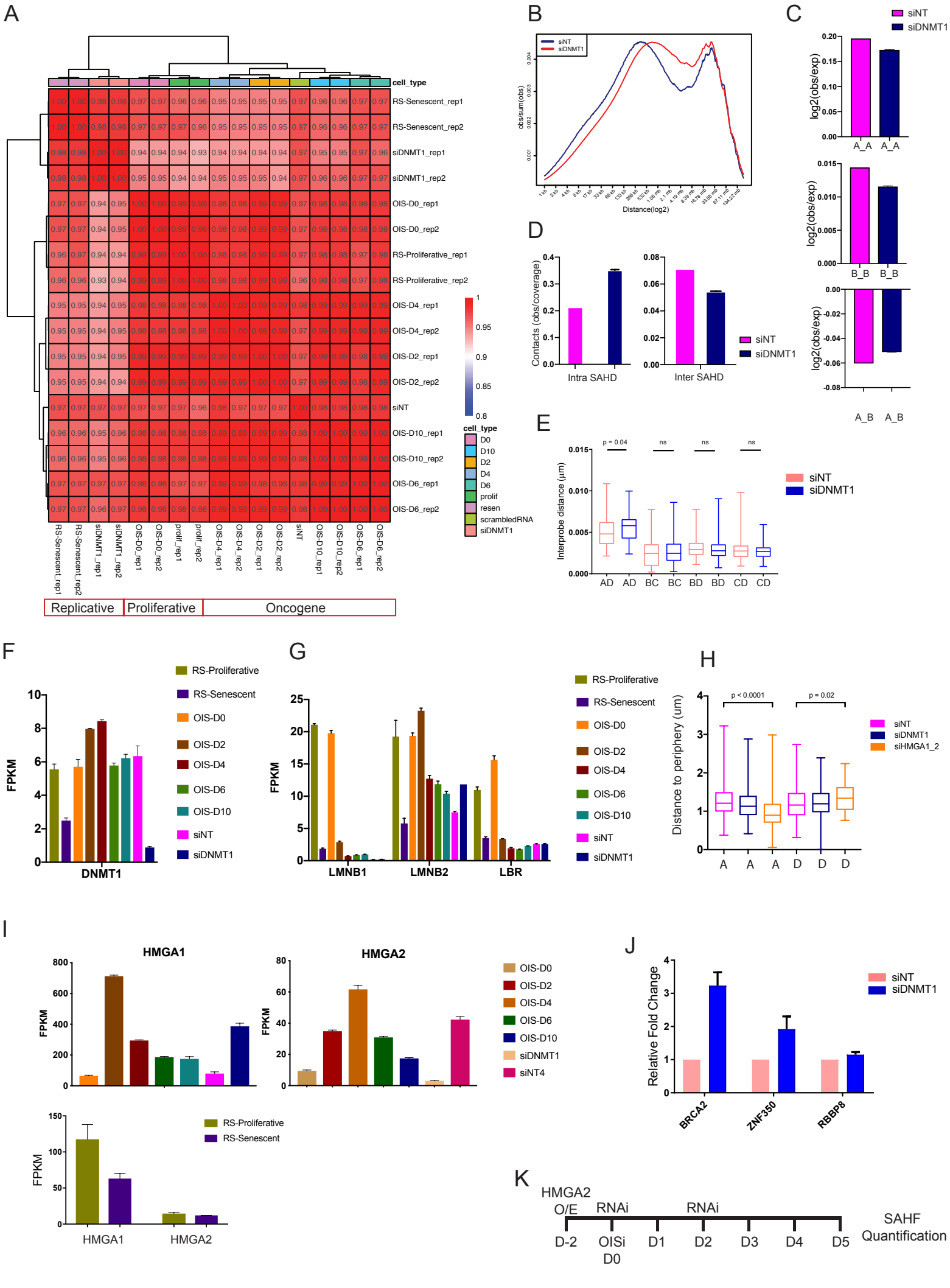

S5. Changes in chromatin architecture in DNMT1 depleted cells under OIS conditions, Related to Figure 5.

(A) Pairwise Pearson's correlation between Hi-C samples (at 100Kb resolution and considering only contacts separated by at least 100Kb and not more than 2.6Mb). (B) Contact probability over distance. Lines: mean values from biological replicates. (C) Intra and Inter compartment contact enrichment from OIS and RS samples. Data represented as bar plot showing the mean ± SD. (D) Quantification of contacts within and between SAHDs in siNT and siDNMT1 treated cells. (E) Boxplot of inter-probe distances form Figure 5D, normalised by mean volume. Statistical significance is calculated using Mann-Whitney test. (F) DNMT1 expression represented as the mean ± SD of three biological replicate RNA-seq experiments for RS-Proliferative, RS-Senescent samples, OIS-D0, OIS-D2 and OIS-D4 samples. For OIS-D6, OIS-D10, NT depleted and DNMT1 depleted samples, expression represented as the mean ± SD of two biological replicate RNA-seq experiments. (G) LMBB1, LMNB2 and LBR expression represented as the mean ± SD of three biological replicate RNA-seq experiments for RS-Proliferative, RS-Senescent, OIS-D0, OIS-D2 and OIS-D4 samples. For OIS-D6, OIS-D10, NT depleted and DNMT1 depleted samples, expression represented as the mean ± SD of two biological replicate RNA-seq experiments. (H) Quantification showing the distance of the SAHD - A and non-SAHD - D probe from the nuclear periphery. Data represented as box plots. Statistical significance is calculated using Mann-Whitney test. (I) HMGA1 and HMGA2 expression represented as the mean ± SD of three biological replicate RNA-seq experiments for OIS-D0, OIS-D2, OIS-D4, RS-Proliferative and RS-Senescent samples. For D6, D10, NT and DNMT1 expression represented as the mean ± SD of two biological replicate RNA-seq experiments. (J) Relative fold change expression of BRCA2, ZNF350 and RBBP8 gene normalised to GAPDH expression levels. The data represents the mean and SD from 3 independent replicates. (K) Schematic overview of the HMGA2 rescue experiment. OISi (oncogene induction). RNAi (administration of siRNA). 2 days before oncogene induction (D -2), Day 0 (OIS-D0) to Day 5 (OIS-D5). HMGA2 over expression (O/E) at 2 days before ois induction ((D (-2)).

Supplementary Figure 6

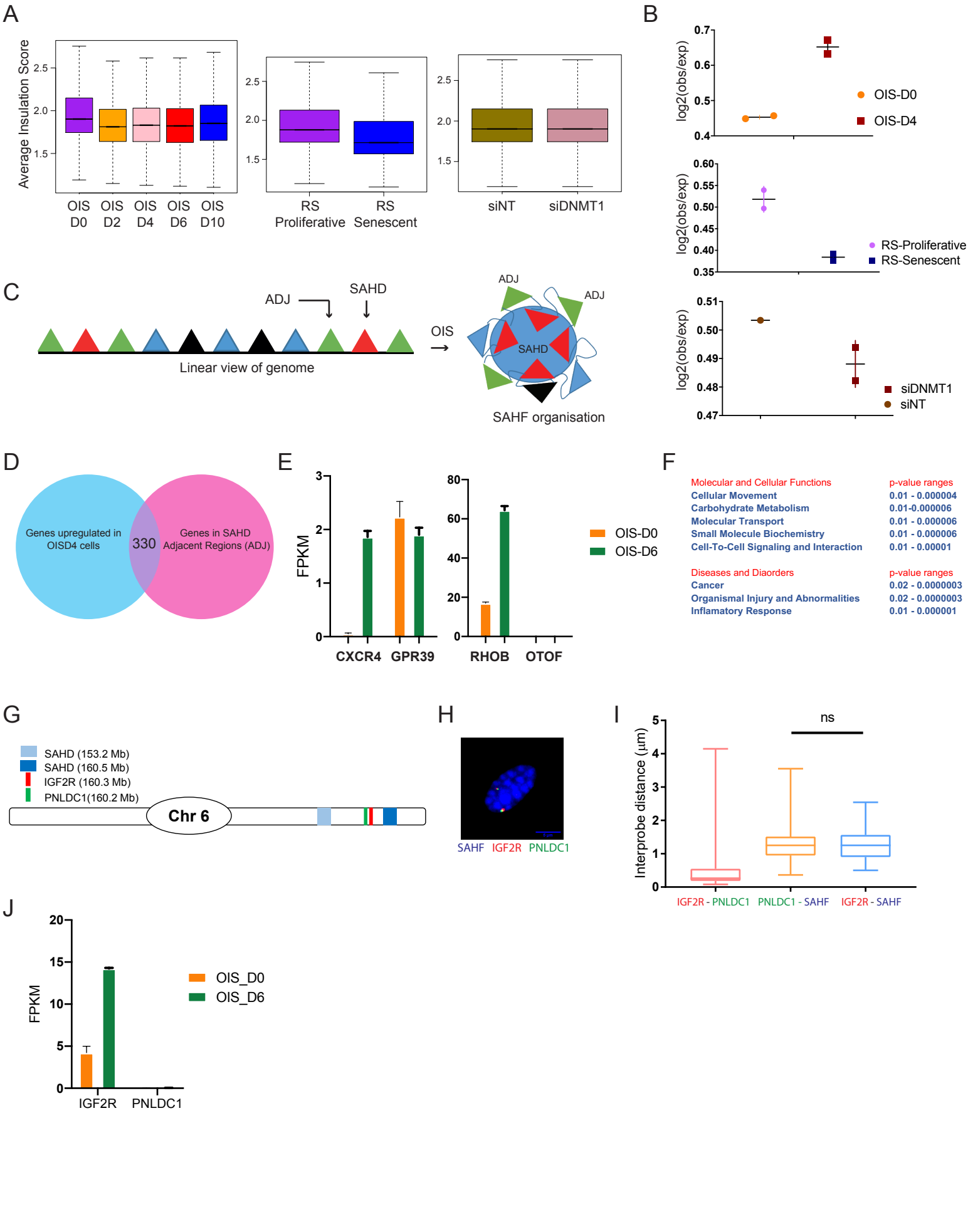

S6. SAHF formation leading to TSS-TSS interaction in a specific subset of genes, Related to Figure 6.

(A) Global insulation represented as box plot in OIS, RS, NT and DNMT1 depleted samples. (B) Quantification of the contact strength between pairs of inter-TAD active TSS. Data are represented as a scatter dot plot showing the mean ± SD. (C) Schematic representation of the SAHD specific gene expression analysis. The linear view of genome displays a representative view of the SAHDs and other regions including the SAHD adjacent regions (ADJ). After oncogene induction, the genome being organised into SAHFs, with SAHDs aggregated in the centre. (D) The overlap between genes upregulated in OIS-D4 (OIS-D4 vs OIS-D0) and genes that fall in ADJ region. (E) CXCR and RHOB expression represented as the mean ± SD of three biological replicate RNA-seq experiments for OIS-D0 and two replicate RNA-seq experiments for OIS-D6. (F) Gene ontology analysis of genes in SAHD specific ADj genes. (G) Schematic representation of the location of FISH probes on chromosome 6. (H) Representative 3D-DNA FISH images (z-slice) from OIS-D6 samples with IGF2R and PNLDC1 probes. Scale bar = 5 μm. (I) Quantification showing the distance of the within the FISH probe sets and between the DAPI marked SAHF body and FISH probes. Data represented as box plots. Statistical significance is calculated using Mann-Whitney test. (J) IGF2R and PNLDC1 expression represented as the mean ± SD of three biological replicate RNA-seq experiments for OIS-D0 and two replicate RNA-seq experiments for OIS-D6.